AADE-14-FTCE-02

Tailoring Thermal, Mechanical, and Physical Properties of Degradable Polymers for Downhole Applications

Feng Liang, formerly Halliburton; B.R. Reddy and Philip D. Nguyen, Halliburton

Abstract

Hydrolytically degradable polymers, typically polylactic acid, have been applied in recent years in various oilfield applications, such as fluid-loss control, fluid diversion, and filter-cake removal. However, the use of these polymers is limited by several challenges, such as size distribution restrictions and temperature limitations.

This paper addresses the shortcomings of the currently used degradable polymers. A laboratory study was conducted modifying the amorphous polylactic acid to obtain the desired physical, mechanical, and thermal properties for meeting application specifications, and to broaden such applications over an extended temperature range. The polymer modifications have been achieved through melt blending with various additives, such as plasticizers, reinforcing agents, etc.

In addition to fluid-loss control or fluid diversion applications, additional applications discussed include coating applications, particularly coating onto proppants or gravel pack sand and downhole tools, such as sand control screens to form a temporary protective coating during downhole placement for gravel packing or frac-packing treatment applications. In one set of experiments, sand was coated with molten modified polymers at different levels. Testing was performed to demonstrate the diverting effects of the coated sand in a lower temperature range and compared with non-modified degradable polymer. For a second set of experiments, polymeric discs were molded by compression molding and subjected to fluid pressures at elevated temperatures. Testing of the novel polymer discs to withstand fluid pressures and temperatures encountered under downhole conditions was performed.

Introduction

Controlling fluid flow rates into or out of a subterranean formation is an ubiquitous operation during the production of hydrocarbons. Some of the examples where manual intervention is undertaken to control fluid flow rates into and out of a subterranean formation or a wellbore are fluid-loss control of wellbore treatment fluids into the formation; reduction of the flow of water from the formation into the wellbore; increasing the permeability or "conductivity" of proppant bed in a fracturing operation; acid cleanup of near wellbore (NWB) formation damage to reestablish or enhance hydrocarbon flow rates; enhanced oil recovery (EOR); temporary plugging for diversion of treatment or fracturing fluids to change or increase treated or fractured area; or removal of water-blocks in a gas well. In some applications, for example, reduction of produced water, the fluid flow control intervention is intended as a long-term ('permanent") solution. In other cases, the intervention is intended to be temporary, for example temporary plugging and diversion of treatment fluids, and the fluid flow control agent is designed to be removable either by a separate treatment or by its inherent degradability. An example of the former case is placement of a particulate material in a non-solvent and its subsequent removal by exposure to suitable solvent.[1] An example of the latter case is the use of water-degradable polymers, such as polyesters and polyimides.[2-6] Fluid flow control materials can include particulate materials (degradable, or acid soluble or hydrocarbon or water soluble) that are either suitably sized for forming a filter cake with minimized permeability, or capable of swelling in a treatment fluid, crosslinked polymer gels, relative permeability modifiers, or viscosifying polymers. A variety of fluid flow control materials have been used in the field, including foams, oil-soluble resins, acid-soluble particulates, superabsorbent materials, graded salt slurries, linear viscoelastic polymers, degradable polymers, and metal-crosslinked polymers. Fluid flow control materials function by a variety of mechanisms, including filter cake formation, plugging of pores, fractures or channels, and by adsorption on pore surfaces.

Even in cases where all efforts have been made to maximize hydrocarbon production from the formation by removing formation damage, actual hydrocarbon production rates can be less than expected when the well is put on production, or, more often, production rates decline at an abnormally fast rate, requiring remedial operations or stimulation of new areas. While there can be many causes for excessive production rate decline, sand and fines production along with hydrocarbon is often believed to contribute to decreased oil production. Produced sand and fines can decrease proppant pack conductivity by blocking the porosity in the proppant bed. Recent efforts to mitigate proppant pack conductivity reduction include approaches focusing on designing proppant placement techniques that provide high initial conductivity. Degradable polyester particulates have

been applied in hydraulic fracturing treatments to increase effective fracture conductivity by enhancing generation of multiple fracture networks in tight formations. [5,7]

In cases where gravel pack completions and screen completions are employed for sand control, plugging of openings in the screens or gravel pack is also believed to contribute to declines in production rates. To maximize efficiency and long-term performance of screens and slotted liners, many techniques have been employed to minimize clogging of well screens and slotted liners during storage against corrosion and during the placement phase against plugging by particulate materials present in the wellbore, such as drill cuttings, or in the completion fluids. These techniques primarily involve coating of the equipment with a protective layer of materials, which can be selectively removed subsequent to placement. Examples of such materials include waxes, solid surfactants, thermoplastic resins, low melting alloys, acid soluble materials, oil soluble resins, and numerous other materials. [8-16] Methods of selectively removing the protective coating include heating, using suitable solvents, or treatment with acids, among others. More recently, degradable thermoplastic polyesters of polylactide type have been used to coat the sand screen equipment to provide protection against corrosion during storage and to prevent clogging of the screen openings during placement. [17-21] Exposure to aqueous fluids downhole degraded the polymer by means of hydrolysis after placement, exposing the openings in pristine condition ready to filter out produced sand. Other benefits of coated sand screens include use of the coated tubular as a wash pipe and the ability of lactic acid generated by coating degradation to dissolve any calcium carbonate in the wellbore used as a filter cake bridging agent.

The potential success of thermoplastic degradable polymeric materials in a variety of situations to increase efficiency of wellbore operations, such as fracturing, and hydrocarbon production rates, has been amply demonstrated both in the laboratory as well as in the field, as described. For these applications, the degradable polymers have been used either in the particulate form (e.g., diversion applications) or as surface coatings deposited on a tool from molten polymer (e.g., sand control applications). Current commercialization efforts using the degradable materials might not have realized the full potential of the materials because of a lack of understanding of how the material properties can be manipulated by changes to material composition.

The objective of the present work is to incorporate additives into the degradable polymers by melt blending to either lower the glass transition temperature to improve processability of the polymer melt for improved ease of coating onto particulate materials, or to enhance mechanical properties for improved fluid-loss properties of coated sand control screens under mechanical and thermal stresses without detrimentally impacting the degradability of the polymers. The latter property enhancement is also expected to enhance the grindabilty of the materials to desirable particle sizes, which is often difficult to accomplish because the mechanical heat generated by the grinding process softens the materials and makes the grinding process difficult unless cryogenic techniques are used to precool the solid before grinding. The particle size optimization of fluid-loss control additives is very important to effectively control the permeability of the filter cake formed by the particulate materials and can require multimodal particle size distribution. The "modality" of a polymeric material generally refers to the number of discrete ranges for the particle sizes in a mixture of particles. For example, a "monomodal" polymeric material refers to a material that comprises molecules having particle size distributions within a single range; whereas, a "multimodal" polymeric material refers to a material that comprises at least two sets of polymer particles having different average particle sizes. In practice, multimodal particulates are generally better at fluid-loss control because it is not always possible to predict the exact sizes of the pore spaces either in the filter cake or in the permeable formation against which the filter cake is deposited.

To lower the glass transition temperatures, several plasticizers are melt blended into amorphous polylactide (PLA); and, to enhance mechanical properties of PLA, highly crystalline polylactide is melt blended into an amorphous PLA polymer as a degradable reinforcement additive.

Experimental Methods

Material Preparation and Characterization

Plasticized PLA Materials. Blending experiments were performed using a Brabender twin-screw mixer. The mixing chamber was preheated to 135°C. About 45 grams (g) of amorphous polylactic acid were loaded into the mixer, followed by specified amounts of plasticizer or reinforcing polymer. The melt was blended for 2 min at a rotor speed of 100 rev/min. Then the mixture was taken out and ground into 1-mm sized particles. In the case of melt blended plasticized PLA composition for sand coating applications, approximately 45 g of amorphous polylactic acid were loaded into the mixer, followed by 6.75 g (15 parts per 100 of resin (PHR) or wt%) of tributyl citrate. The melt was blended for 2 min at a rotor speed of 100 rev/min. Then, the mixture was taken out and ground into 1-mm sized particles.

Differential Scanning Calorimetry (DSC). DSC analysis was performed on a Q200 equipment from TA Instruments on a control sample of amorphous polylactic acid and its plasticized blends. All DSC scans were conducted in hermetically sealed pans, under N2 atmosphere, using approximately 10 mg of material. The scans were run from -50 to 200°C (10°C/min), cooled back down to -50°C (5°C/min), and then reheated back to 200°C (10°C/min). All the glass transition temperatures reported were determined from the first heating cycle.

Coating Methods

Sand Coating. Plasticized PLA coated proppant particulates were prepared by coating 20/40-mesh sand with 15 wt% of the plasticized PLA. Then, 60 g of the plasticized PLA was added to 400 g of 20/40-mesh sand (proppant particulate) heated to 280°C for 30 min and vigorously stirred. After the mixture was well stirred, cool water was added to cause the degradable plasticized PLA to deposit onto or adhere to the sand and form degradable plasticized PLA coated proppant particulates. The plasticized PLA coated proppant particulates were filtered and air dried. A control sample was prepared by coating unplasticized PLA on to the sand at the same wt%.

Sand Pack Testing. A 1-in. inside diameter (ID) cell was packed with 150 g of 20/40-mesh sand that was coated with 15% unplasticized amorphous PLA, or 15% plasticized PLA, and tapped down with a packing rod. A diagram of the cell and test set up are shown in Fig. 1 (the cell was vertical during the run). Preheated tap water was flowed through the cell at rates of 1.3, 1.5, and 1.7 gal/min by increasing the flow rates in incremental steps. When the compression of the sand pack was taking place, it was necessary to adjust the pump speed to maintain at a constant flow rate. The pressure, flow rate, bath temperature, and temperature at the cell were recorded.

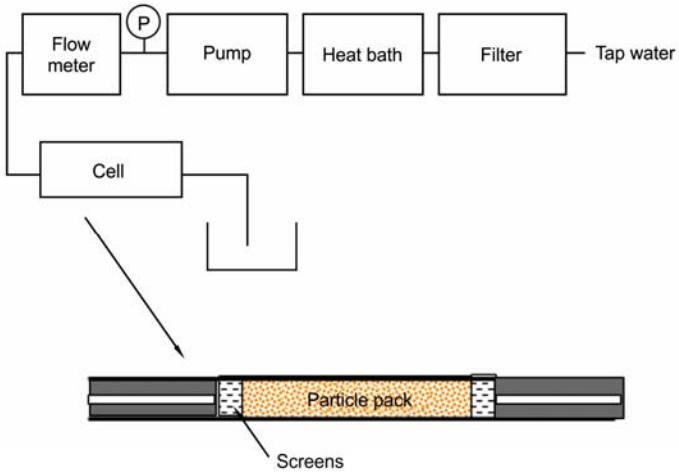

Fig. 1—Test setup and flow cell.

Sandscreen Applications. During each test, amorphous polylactic acid was molded into a 2.5- × 0.25-in. (diameter × thickness) wafer. Next, the wafer was placed into a high-pressure/high-temperature (HP/HT) cell that contained a metallic disc-shaped bottom plate of dimensions 2.5- × 0.25-in. (diameter × thickness) with a hole (0.44- or 0.25-in. diameter) at the center. The HP/HT cell was filled with 250 mL of tap water. The set up was then heated to a set temperature ranging from 54°C (130ºF) to 82°C (180ºF) for 1 hr. After the elapsed time, pressure was applied to test the extrusion properties of the sample wafer.

Results and Discussion

Material Formulations and Structure-Property Relationships. Table 1 lists the formulations of the amorphous PLA with different plasticizers and their glass transition temperature measured by DSC.

Table 1—Effect of Plasticizers on Glass Transition Temperature (Tg) of Amorphous PLA

Expt No.	Plasticizer PHR/100 PHR Amorphous PLA		Tg (°C)
	Plasticizer	PHR	
1	N/A	N/A	58
2	Lactide	18	27
3	Lactide	30	20
4	Lactide	40	14
5	Dibutyl Phthalate	24	12
6	Dibutyl Phthalate	30	4
7	Triacetin	30	2
8	Tributyl Citrate	15	33
9	Tributyl Citrate	30	6
10	Diethyl bis(hydroxymethyl)malonate	30	12

The results in Table 1 illustrate that, at constant wt% of plasticizers, the following decreasing order of their effectiveness for lowering Tg was observed: triacetin > dibutyl phthalate > tributyl citrate > diethyl bis(hydroxymethyl)malonate > lactide. Non-plasticized PLA with a Tg of approximately 50°C is a very brittle material similar to polystyrene. Plasticization is helpful for increasing flexibility, reducing brittleness, improving impact strength, improving coating quality, and reducing tendency of coatings to crack and improve melt processability (lower melt viscosity). The presence of plasticizers does not affect the degradability of the polymers and can sometimes increase degradability. Additionally, addition of plasticizers facilitates lower temperature applications because of the decreased glass transition temperatures.

The DSC curves of the control amorphous PLA material used in this study is shown in Fig. 2. It shows a glass transition temperature at 58°C (136°F).

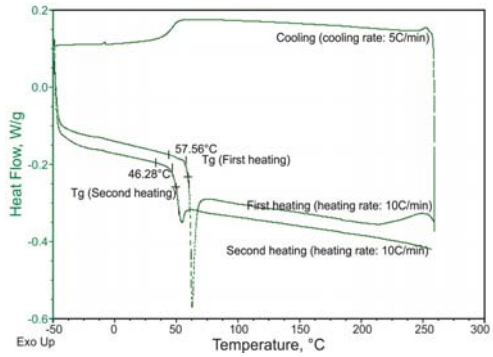

Fig. 2—DSC curves of amorphous PLA alone.

DSC traces recorded for the above amorphous PLA plasticized with 15 PHR Tributyl Citrate is shown in Fig. 3. Tg was determined to be 33°C.

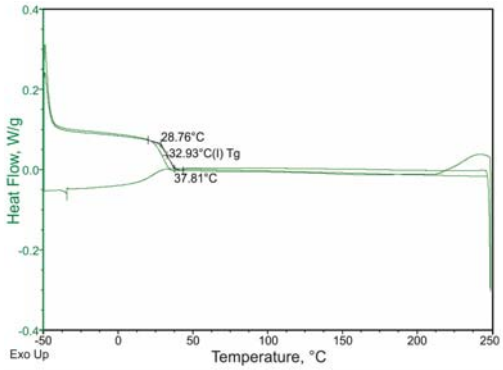

Fig. 3—DSC traces recorded for plasticized PLA (made with 15 PHR Tributyl Citrate) in a heat-cool-heat cycle. Tg was determined to be 33°C.

PLA Coated Sand for Fracturing/Diversion Applications. The objective of this study was to use PLA coated sand for use as proppant sand or gravel pack sand. At the end of a fracturing or gravel packing operation, continued exposure of the sand to aqueous fluids will degrade the polymer and leave conducting channels. In the case of gravel packing operations, this will serve as a protective barrier against potential plugging sand porosity by particulates present in the wellbore, such as drill cuttings. During fracturing operations, the coated sand can serve to divert the fracturing fluids in other areas. The procedure for coating the sand with PLA is provided in the "Experimental" section of this paper. The following fluid flow experiments were performed with PLA coated sand.

Test 1. The cell was packed with 150 g of 20/40-mesh sand coated with 15% amorphous PLA. At a temperature of 110°F, with a flow rate of 1.3 gal/min, a slight pressure increase was observed. Then, the rate was increased to 1.5 and 1.7 gal/min, and similar phenomena was observed. Only slight pressure increase in the range of approximately 100 psi over an entire flow measurement duration of 25 min was observed (Fig. 4).

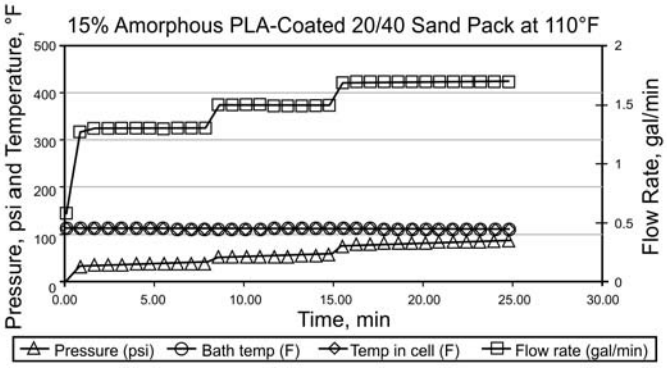

Fig. 4—Cell testing of 15% amorphous PLA coated 20/40 sand pack at 110°F.

Test 2. The cell was packed with 150 g of 20/40-mesh sand coated with 15% plasticized PLA. At a temperature of 110°F, with a flow rate of 1.3 gal/min, a dramatic pressure increase was observed. Within 8 min, the pressure reached 520 psi, which indicated the plugging of the sand pack (Fig. 5). This was believed to have occurred because 110°F (43°C) was above the glass transition temperature (Tg) of the plasticized PLA material (91°F, 33°C), causing the plasticized PLA to become soft at the treating temperature (110°F, 43°C), causing the coatings of the sand grains to fuse and plug the sand pack.

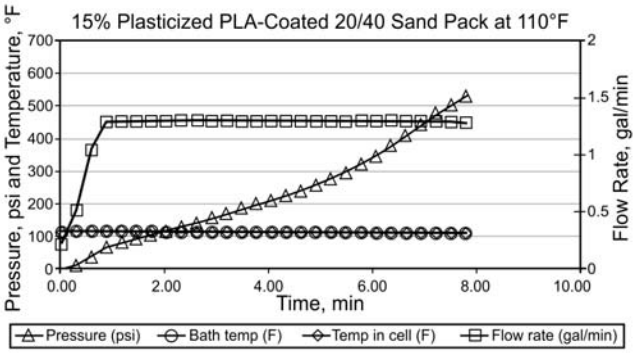

Fig. 5—Cell testing of 15% plasticized PLA coated 20/40 sand pack at 110°F.

Test 3. The cell was packed with 150 g of 20/40-mesh sand coated with 15% amorphous PLA. At a temperature of 140°F, with a flow rate of 1.3 gal/min, a dramatic pressure increase was observed. Within 5 min, the pressure reached 520 psi, which indicated plugging of the sand pack (Fig. 6). The flow rate decreased slightly at the same time. Because the Tg of amorphous PLA was determined to be 58°C (136°F), the treating temperature of 140°F was slightly higher than the glass transition temperature, causing the PLA to be significantly fused and compressed under pressure at this temperature.

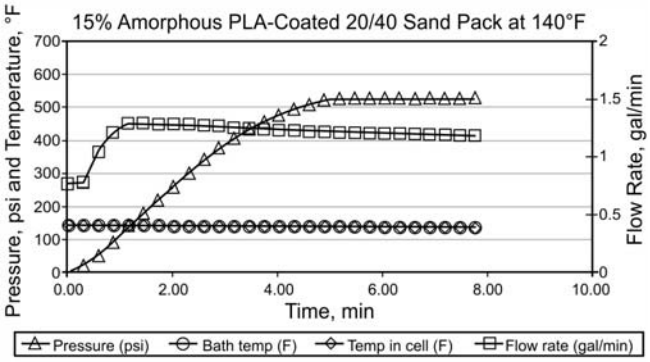

Fig. 6—Cell testing of 15% amorphous PLA coated 20/40 sand pack at 140°F.

Test 4. The cell was packed with 150 g of 20/40-mesh sand coated with 15% plasticized PLA. At a temperature of 140°F, with a flow rate of 1.0 gal/min (note the flow rate of 1.3 gal/min could not be reached because of plugging), a dramatic pressure increase was observed. Within 1 min, the pressure reached 520 psi, which indicated plugging of the sand pack (Fig. 7). At the same time, the flow rate quickly dropped from 1.0 to 0.65 gal/min. The plugging time was shorter than Test 3, which was packed with 15% amorphous PLA coated 20/40-mesh sand pack.

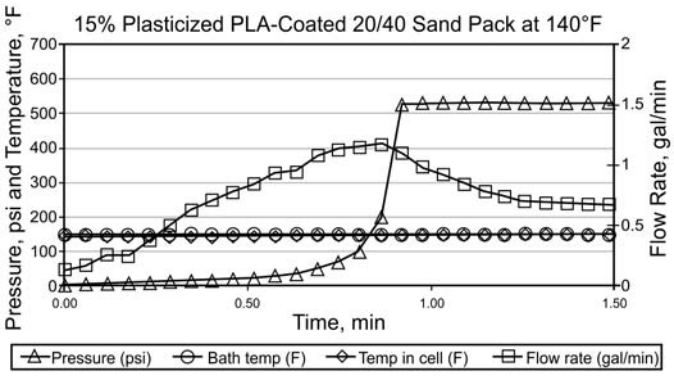

Fig. 7—Cell testing of 15% plasticized PLA coated 20/40 sand pack at 140°F.

The results from the four tests are summarized in Table 2. The results clearly show that, when the test temperatures are significantly higher than the glass transition temperature of the polymer coating, very rapid fluid-loss control can be realized attributed to fusing of polymer coatings of individual sand particles. This observation implies that plasticized PLA coated proppant can provide effective fracturing fluid diversion to other areas, enabling even distribution of proppants or enhancing creation of new fractures. Additionally, on degradation of polymer coating, proppant beds with enhanced conductivity attributed to the formation of wider flow paths left behind by degraded polymer can be realized.

Table 2—Fluid-Loss Control Differences for Amorphous and Plasticized Amorphous PLA Coated Sand Packs

PLA	Temp (°F)	Test Temp Tg (◦F)	Time to Reach 500 psi
Amorphous PLA	110	-26	Did not reach pressure in 25 min
Platicized Amorphous PLA	110	-26	8 min
Amorphous PLA	110	+4	5 min
Plasticized Amorphous PLA	110	+4	1 min

Sand Screen Coatings. The extrusion characteristics of amorphous polylactic acid were tested at different temperatures and pressures using molded wafers. The testing conditions for each wafer are shown in Table 3.

Table 3—Parameters for Simulation Testing of Sand Screen Coated with Amorphous PLA

Simulation Test No.	1	2	3	4
Metal Disc Hole Diameter (in.)	0.44	0.25	0.25	0.25
Temp, °C (ºF)	82 (180)	82 (180)	65 (150)	54 (130)
Pressure (psi)	100	140	200	200

The results of Simulation Test 1 are shown in Fig. 8A through 8D. These figures show that an amorphous polylactic acid wafer deforms and extrudes at 82°C (180ºF) and 100 psi differential pressure. Fig. 8A through 8B represents the bottom views of the wafer. These figures show extrusion of polylactic acid from the center hole of the metal disc; and the wafer was blown out after it was exposed to 82°C (180ºF) and 100 psi in a very short time. Fig. 8C through 8D shows top views of the wafer. The results of Test 2 are shown in Fig. 9A through 9D. Fig. 9A through 9B is similar to 8A through 8B as the bottom views of the wafer shows extrusion of polylactic acid from the center hole of the metal disc; and it was blown out after being exposed to 82°C (180ºF) and 140 psi in a very short time. Fig. 9C through 9D shows top views of the same wafer in Fig. 9A through 9B. Results of Test 3 are shown in Fig. 10A through 10D. Fig. 10A through 10B shows protrusion and extrusion of the amorphous polylactic acid from the center hole of the metal disc after being treated at 65°C (150ºF) and 200 psi for 2 hr. Fig. 10C through 10D represents top views of the tested wafer. In Tests 1 through 3, the temperature of the HP/HT cell is greater than the glass transition temperature (~136°F) of amorphous polylactic acid. Test 4 results are shown in Fig. 11A through 11D. Fig. 11A through 11B shows bottom views of the wafer after it was exposed to 54°C (130ºF) and 200 psi for 2 hr. Slight protrusion of the center hole can be observed. The wafer, however, does not display grids from the cell lid as the temperature did not exceed the glass transition temperature. Fig. 11C through 11D shows top views of the tested wafer.

These figures show that an amorphous polylactic acid can deform under relatively modest temperatures and pressures. In Tests 1 through 3, the amorphous wafers were subjected to temperatures above its Tg and demonstrated poor mechanical properties, including deformation and extrusion. In Test 4, the amorphous wafer was subjected to a temperature below its Tg and thus did not deform to the shape of the cell lid, but did show some deformation.

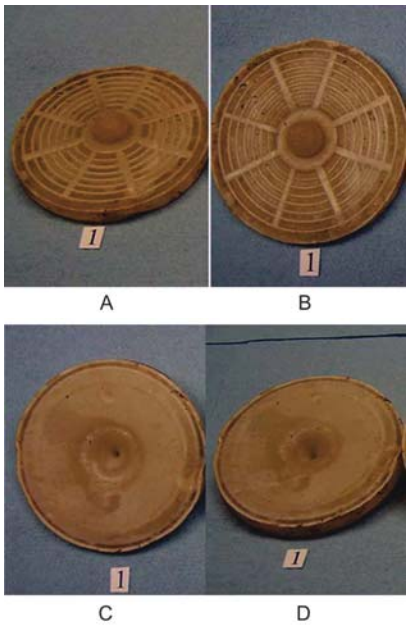

Fig. 8—Amorphous PLA wafers after testing in HP/HT cells with a 0.44-in. hole at 180°F under 100 psi.

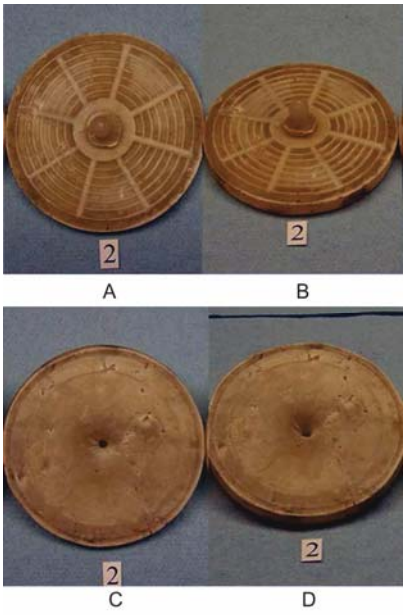

Fig. 9—Amorphous PLA wafers after testing in HP/HT cells with a 0.25-in. hole at 180°F under 140 psi.

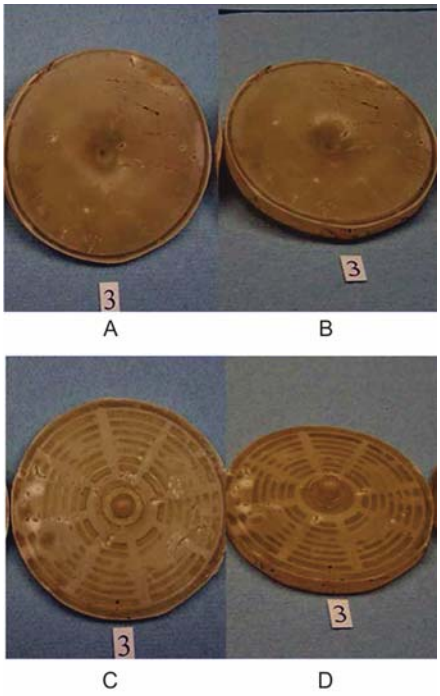

Fig. 10—Amorphous PLA wafers after testing in HP/HT cells with a 0.25-in. hole at 150°F under 200 psi for 2 hr.

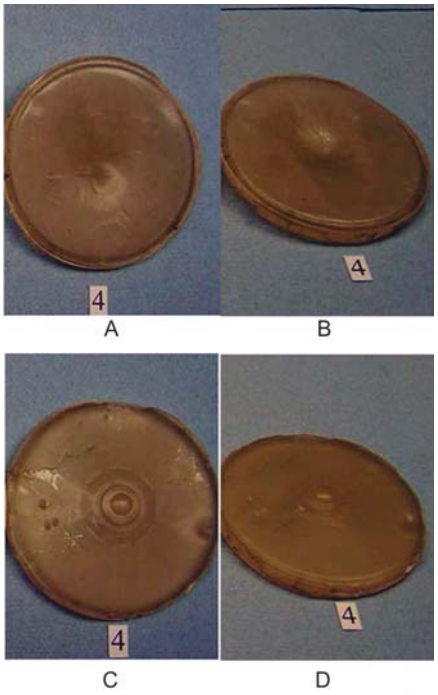

Fig. 11—Amorphous PLA wafers after testing in HP/HT cells with a hole of 0.25-in. at 130°F under 200 psi or 2 hr.

This example illustrates, among other things, that amorphous polylactic acid generally has poor mechanical properties, such as deforming and extruding under relatively low temperatures and pressures.

In this example, an amorphous polylactic acid wafer was tested with a wrapped screen under conditions closely simulating real downhole conditions (PLA-pipe with 0.25-in. ID and 0.15-in. thickness-wrapped screen). The screens were installed into a test fixture. The amorphous wafer and wrapped screen were tested in a HP/HT cell at 82°C (180°F) and 200 psi. The wrapped screen was placed behind the metal disc.

The result of the test is shown in Fig. 12. In this figure, the amorphous polylactic acid wafer did not hold pressure, as extrusion can be clearly observed in the first metal grid. However, the extrusion never reached the wrapped screen. It only took a few minutes for the integrity of the PLA wafer sample to give away and release water from the cell.

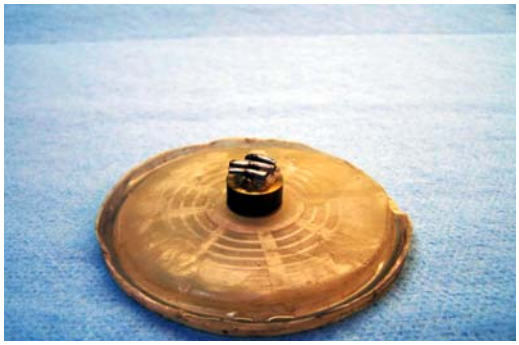

Fig. 12—Amorphous PLA wafers after testing in HP/HT cells with a 0.25-in. hole and wrapped screen at 180°F under 200 psi.

This Example (Fig. 12) shows, among other things, the failure of amorphous polylactic acid installed with a screen to resist deformation and extrusion under simulated downhole conditions.

Reinforced PLA. The DSC curves of the semi-crystalline PLA material was shown in Fig. 13. Amorphous PLA shows a glass transition temperature at 58°C (136°F) (Fig. 1), while the crystalline PLA shows a glass transition temperature at approximately 60°C (140°F) and the melting point at approximately 165°C (329°F) (Fig. 13). The composite comprising 70% of the amorphous polylactic acid and 30% of the semi-crystalline polylactic acid powder was mixed in a Brabender® mixer at 135°C (275°F). The mixture shows a glass transition temperature at 52°C (126°F) and a melting peak at 167°C (332°F), which is attributed to the crystalline structure of crystalline PLA (Fig. 14). The resulting mixture was stiffer than neat amorphous polylactic acid alone. The mixture was then heated in a 204°C (400°F) in an oven for 1 hr. This heated mixture was observed to be much thinner fluid and easier to pump than the neat amorphous polylactic acid heated under the same conditions.

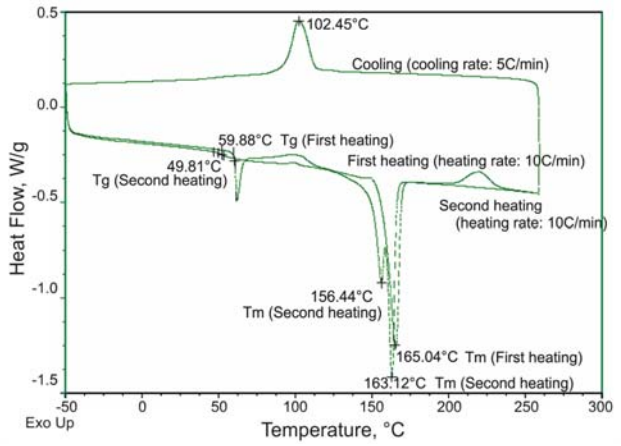

Fig. 13—DSC curves of crystalline PLA.

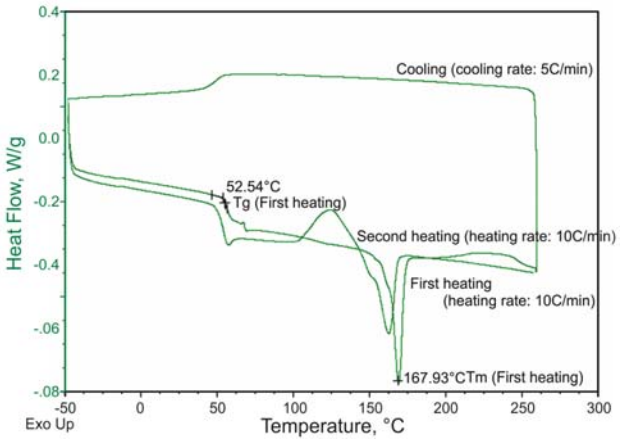

Fig. 14—DSC curves of the composite (70% amorphous PLA, 30% crystalline PLA powder).

This result illustrates, among other things, the ease of manufacturing involved in the making of reinforced amorphous polylactic acid. The advantage of this mixture is that it should provide better mechanical properties than neat amorphous PLA at elevated temperature (but lower than the melting point of the neat crystalline PLA), such as 82°C (180°F), while being easier to pump than neat amorphous PLA at temperatures higher than the melting point of the neat crystalline PLA, such as 204°C (400°F). This provides the advantage of both pumping ability to make the coating at higher temperature, as well as the better mechanical properties at a lower operation temperature. The reinforced amorphous polylactic acid is also easier to handle than crystalline polylactic acid, particularly in large scale scenarios. Overall, this composite material should provide the advantage of both pumping ability to make a coating at higher temperature than crystalline polylactic acid as well as providing better mechanical properties than amorphous polylactic acid.

The reinforced amorphous PLA material showed quick degradation as well as better mechanical properties in comparison to either crystalline PLA or amorphous PLA. The material did not show any brittleness as expected for a well plasticized brittle polymer. Additionally, because of its low Tg

(~58°C or 137°F), the amorphous PLA will deform above its glass transition temperature and will not hold much differential pressure. By reinforcing amorphous PLA with crystalline PLA particles, the resulting composites have shown dramatic enhancements in mechanical properties over the neat amorphous PLA at elevated temperature. The reinforced material can be used in various oilfield applications where quick degradation as well as better mechanical properties are desired in downhole conditions. An example of such application where reinforced PLA can be used is the screen coating in gravel packing applications. The advantage of coating the screen with this material is to protect the screens from damage as they are inserted into the wellbore. Once in the wellbore, they will release acids by hydrolysis of PLA to clean up potentially plugging materials, such as calcium carbonate present in the filter cake. Additionally, the coated screen can act as a wash pipe when chemicals are pumped through the screen. For this purpose, the coating materials might require certain strength/mechanical properties at downhole conditions. This material can also be used in other applications (e.g., as diverting materials, components of fluid loss pill, self-degrading temporary plugs, etc.). These applications require the material to degrade after a delay, while possessing sufficient mechanical strength to withstand the differential pressure. Such materials are also expected to be easier to mechanically grind to desired particle sizes with desired multimodality without using cryogenic techniques.

To demonstrate the effectiveness of reinforced amorphous PLA to withstand high differential pressures at elevated temperatures, the reinforced polymer was molded into wafers (dia. × L: 2.5 × 0.25 in.). The PLA wafer was assembled into a HP/HT cell for mechanical stability testing under high temperature and pressure as described previously. The wrapped screen was placed in the HP/HT cell. A 2.5- × 0.25-in. metal disc (diameter × thickness), which contains a 0.25-in. hole in the center was placed on top of the wrapped screen. Next, the reinforced amorphous polylactic acid wafer was placed in a HP/HT cell. The cell was filled with 250 mL of tap water and heated to 82°C (180°F) for 2 hr.

After the elapsed time, the first wafer was subjected to a pressure of 200 psi. Fig. 15 shows the reinforced amorphous polylactic acid wafer after being held at 200 psi for more than 2 hr. The imprints of the HP/HT lid can be seen on the wafer. No extrusion was observed on the wafer. No leaks were detected. This reinforced PLA composite wafer is visibly superior to the amorphous wafers tested under milder test conditions (Tests 1 through 4).

Fig. 15—Reinforced amorphous PLA wafers after testing in HP/HT cells with a 0.25-in. hole and wrapped screen at 180°F under 200 psi for 2 hr.

A second reinforced PLA composite wafer (70% amorphous PLA/ 30% crystalline PLA) with a wrapped screen was subjected to a pressure of 500 psi for 2 hr. Fig. 16 shows the resulting reinforced amorphous polylactic acid wafer after being held at 500 psi for more than 2 hr. The wafer showed no extrusion and a small protrusion in the center (1/4-in. OD × 0.063 in.). No leaks were detected.

Fig. 16—Reinforced amorphous PLA wafers after testing in HP/HT cells with a 0.25-in. hole and wrapped screen at 180°F under 500 psi for 2 hr.

In this example, a slot test was performed on the reinforced amorphous polylactic acid wafer. A wafer of 70% amorphous PLA/ 30% crystalline PLA was molded. The wafer was then tested in a HT/HP cell containing 250 mL of tap water. The wafer was placed inside the cell against a slot model and heated to 180°F for 2 hr. The dimensions of the slot in the disc were 1.5-in. length × 0.065-in. width × 0.125-in. thickness (metal disc in Fig. 17). The wafer was modified to allow the use of a 0.125-in. thick slot model. The thickness of the polylactic acid wafer at the slot was 0.25 in. The lip portion of the wafer was 0.125 in., allowing the combined installation to include the slot model. After the elapsed time, pressure was applied at 500psi against a slot model. The polylactic acid wafer was held under 500 psi for more than 2 hr at 82°C (180°F) with no leaks. An approximately 1.25-in. length × 0.065-in. width × 0.05-in. thickness, a protrusion was observed on the wafer (Fig. 17).

Thus, this example illustrates, among other things, the mechanical strength of reinforced amorphous polylactic acid under relatively harsh temperature and pressure.

Fig. 17—Reinforced amorphous PLA wafers after testing in HP/HT cells with a 1.5-in. length × 0.065-in. width × 0.125-in. thick slot model at 180°F under 500 psi for 2 hr.

Conclusions

The following conclusions can be drawn from this study.

- Plasticization with accompanying lowering of glass transition temperature of amorphous PLA allowed for effective fluid-loss control through sand packs made from polymer coated sand at wellbore temperatures above the glass transition temperatures of the polymer.
- Plasticized materials can be useful in fluid-loss control applications and in fracture fluid diversion applications aimed at uniform distribution of proppant, enhanced conductivity proppant beds, and enhanced fracture complexities.
- Reinforcement of amorphous PLA with semicrystalline PLA allowed for improvement of mechanical properties of the polymer composite, which resisted fluid pressure differentials, even at high temperatures against extrusion because of polymer softening.
- Improved mechanical properties of reinforced amorphous PLA can allow use of materials, such as degradable coating materials for sand control screens and slotted liners etc., to prevent plugging of openings during storage and downhole placement by particulate materials formed because of corrosion inherently present in the wellbore or the treatment fluids.

Acknowledgments

The authors thank Halliburton management for permission to publish this paper and Dr. Rajesh Saini[21-23] and Mr. Brad Todd[21-23] for their contributions to the study.

References

1. Harrison, N.W. 1972. Diverting Agents—History and Applications. *JPT* **24** (5): 593–598. http://dx.doi.org/10.2118/3653-PA.
2. Glasbergen, G., Todd, B., Van Domelen, M., and Glover, M. 2006. Design and Field Testing of a Truly Novel Diverting Agent. Paper SPE 102606 presented at the SPE Annual Technical Conference and Exhibition, San Antonio, Texas, USA, 24–27 September. http://dx.doi.org/10.2118/124141-MS.
3. Solares, J.R., Al-Harbi, M., Al-Sagr, A., Amorocho, R., and Ramanathan, V. 2008. Successful Application of Innovative Fiber-Diversity Technology Achieved Effective Diversion in Acid Stimulation Treatments in Saudi Arabian Deep Gas Producers. Paper SPE 115528 presented at the SPE Asia Pacific Oil and Gas Conference and Exhibition, Perth, Australia, 20–22 October. http://dx.doi.org/10.2118/115528-MS.
4. Potapenko, D.I., Tinkham, S.K., Lecerf, R., Freed, C.N., Samuelson, M.I., Gillard, M.R., Calvez, J.H., and Daniels, J.I. 2009. Barnett Shale Refracture Stimulation Using a Novel Diversion Technique. Paper SPE 119636 presented at the SPE Hydraulic Fracturing Technology Conference, The Woodlands, Texas, USA, 19–21 January. http://dx.doi.org/10.2118/119636-MS.
5. Allison, D., Curry, S., and Todd, B. 2011. Restimulation of Wells Using Biodegradable Particulates as Temporary Diverting Agents. Paper CSUG/SPE 149221 presented at the Canadian Unconventional Resources Conference, Calgary, Alberta, Canada, 15–17 November. http://dx.doi.org/10.2118/149221 – MS.
6. Fuller, M.J. and Still, J.W. 2013. Use of Polyimides in Treating Subterranean Formations. US Patent 7,841,411.
7. Allison, D., Bryant, J., and Butler J. 2013. Hydrocarbon Recovery Boosted by Enhanced Fracturing Technique. Paper SPE 167182 presented at the Unconventional Resources Conference-Canada, Calgary, Alberta, Canada, 5–7 November.

8. Ledlow, Jr. and Sparlin, D.D. 1960. Downhole Protection of Sand Control Screens. Paper SPE 8803 presented at the Fourth Symposium on Formation Damage Control of the SPE of AIME, Bakersfield, California, USA, 28–29 January.
9. Blount, E.M. 1973. Well Treating Process Using Sacrificial Plug. US Patent 3,768,563 (Issued Oct. 30, 1973).
10. Muecke, T.W. and Graham, J.W. 1975. Well Screens. US Patent 3,880,233 (Issued April 29, 1975).
11. Sparlin, D.D. and Kolb, Jr. C.B. 1975. Method of Protecting Well Apparatus Against Contamination During Handling. US Patent 3,905,423 (Issued Sept 16, 1975).
12. Sharp, K.W. and Sparlin, D.D. 1980. Acid Soluble Coating For Well Screens. US Patent 4,202,411 (Issued May 13, 1980).
13. Jones, L.G. 1992. Gravel Packing of Wells With Flow-Restricted Screen. US Patent 5,165,476 (Issued Nov. 24, 1992).
14. Arterbury, B.A. and Cornette, H.M. 1994. Foil Wrapped Base Paipe For Sand Control. US Patent 5,310,000 (Issued May 10, 1994).
15. Cornette, H.M. 1994. Sand Control Screen and Installation Method For Wells. US Patent 5,320,178 (Issued June 14, 1994).
16. Hazen, J.L., Einziger, M.D., and Denton, W.K. 1996. Non-ionic Surfactants With Enhanced Aqueous Dissolution Rates. US Patent 5,567,475 (Issued Oct. 22, 1996).
17. Constein, V.G. 2002. Product for Coating Wellbore Screens. US Patent Publication 2002/0142919 A1 (Publ. Date. Oct 3, 2002).
18. Cooke Jr., C.F. 2011. Method and Apparatus For Delayed Flow or Pressure Change in Wells. US Patent 8,025,104 (Issued Sept. 27, 2011).
19. Cooke, Jr. C.F. 2012. Application of Degradable Polymers in Sand Control. US Patent 8,215,385 (Issued July 10, 2012).
20. Liang, F., Todd, B., Welton,T., and Saini, R. 2013. Method For Improving Coatings on Downhole Tools. WO2013052290 A2.
21. Liang, F., Saini, R., and Todd, B. 2013. Amorphous PLA with Solid Particles for Downhole Applications. US 20130081821 A1; WO 2013052285 A1.
22. Liang, F.. Saini, R.. Todd, B. 2013. Reinforcing Amorphous PLA with Solid Particles for Downhole Applications. US 20130081821 A1; WO 2013052285 A1.
23. Liang, F., Todd, B., Welton, T., and Saini, R. 2013. Methods of Fluid Loss Control, Diversion, and Sealing Using Deformable Particulates. WO 2013052252 A1.